Vacuum Loss Detection of PTC in CSP Plants via Temperature-Sensors

Thomas Kraft[1] [iD], Gregor Bern[1] [iD], Shahab Rohani[1] [iD],
Mark Schmitz[2], and Werner Platzer[1] [iD]

[1] Fraunhofer-Institut für Solare Energiesysteme ISE, Germany

[2]TSK Flagsol Engineering GmbH, Germany

Abstract. The efficient operation of a solar field is an essential factor for the commercial operation of a concentrating solar power (CSP) plant. In addition to predictive control for the highest possible constant outlet temperature at high mass flow, efficient operation also includes early detection of defective components and heat losses. This work presents a method for non-invasive heat loss detection as a strong indication for vacuum losses, based on measured operational data of Andasol III, an operating 50 MW parabolic trough collector (PTC) plant located in southern Spain. To detect vacuum losses via this method, mass flow rate and temperature reduction are determined separately for each individual loop via the analysis of a short-term temperature rise of the heat transfer fluid (HTF) during preheating. While the temperature reduction was measured directly, the mass flow was determined via the thermal time-of-flight (ToF) method using the same installed temperature sensors. By measuring thermal step responses during the preheating of the solar field at nighttime operation, the influence of fluctuating direct normal irradiance (DNI), misalignment of the absorber tubes and an offset in collector focus was circumvented. In the scope of the presented work, single loops were detected, which show a higher heat loss at lower mass flow rate and therefore have an increased probability of a higher vacuum loss. Better localization and early detection of these vacuum losses would allow the corresponding absorber tubes to be renewed at the economically and environmentally best time, improving the efficiency of the solar field and thus the entire CSP plant.

Keywords: Vacuum Loss, Heat Losses, Solar Field Optimization, Mass Flow Measurement, Thermal Time-of-Flight, Concentrated Solar Power (CSP)

1. Introduction

Vacuum losses in evacuated absorber tubes lead to significant degradation of thermal performance of CSP power plants. Due to the absorber tube vacuum losses, especially the convective heat losses increase with time to such an extent, that after some years a complete replacement of the absorber tubes may become economically reasonable. A total loss of vacuum can lead to an increase in glass surface temperature of more than 60 K for the correspondent collector tube [1]. The influence of different hydrogen concentrations and thus reduced vacuum on the total plant efficiency is analyzed in detail by Zoschke et al. [2]. The study shows a decline of 12% in electrical yield for a hydrogen concentration of 30%.

In principle, the vacuum loss can be caused by diffusion of hydrogen as well as by leakage of air. The ingress of air can be both creeping due to microcracks and sudden due to mechanical loads (e.g., damage during cleaning). The air can enter the vacuum between the absorber tube and the glass envelope either through the glass surface or through a leaky glass-to-metal connection. Although the design and the material connections between steel and glass are advanced, studies show that the vacuum efficiency is decreasing with time [3]. Figure 1 schematically shows the structure of an absorber tube and the different types of vacuum losses.
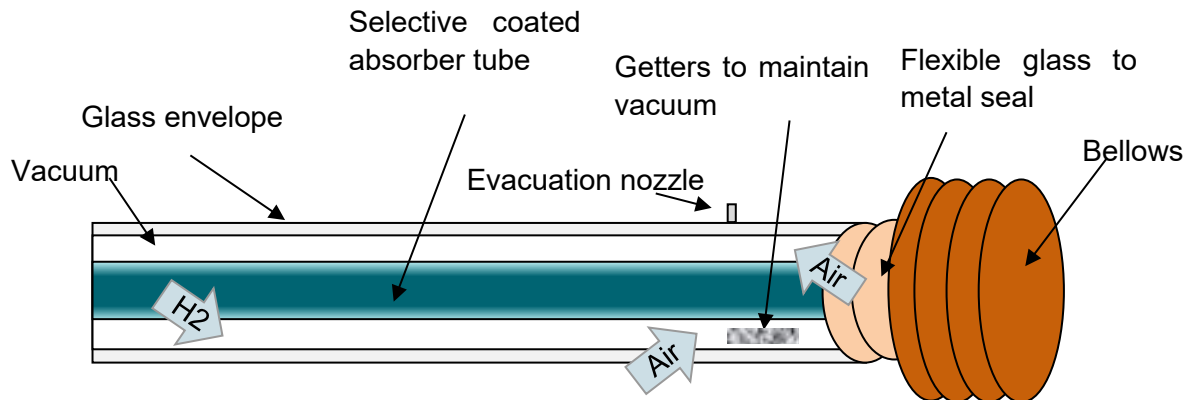

Figure 1. Scheme of an absorber tube and possible types of vacuum loss, inspired by [4].

Since vacuum loss significantly influences the efficiency of the solar field and thus of the entire power plant, its early detection is important for efficient power plant operation. Due to the complex localization of vacuum loss via measuring the glass surface temperature using additional temperature sensors or by infrared cameras, there is a need for a simple and cost-effective method for vacuum loss detection.

2. Methodology

For the localization of loops with an increased probability of vacuum loss, two different aspects were analyzed: mass flow and temperature reduction of HTF within the loops. By carrying out the measurement of thermal step responses during the preheating of the solar field at nighttime operation, the influence of fluctuating DNI, soiling, misalignment of the absorber tubes and offset in the collector focus was strongly reduced or even completely prevented.

2.1 Heat loss estimation

Figure 2 schematically shows a loop of a CSP plant with PTC, where the loop consists of four solar collector assemblies (SCA). The loop has five temperature sensors, four of which (A-D) are located in the center of the SCAs and one temperature sensor at the end of the loop (E). In the figure on the left, the temperatures measured at these sensors are shown for an exemplary loop on an exemplary day of a commercial CSP plant. The thermal step response due to the preheating of the solar field around 6 o'clock in the morning is clearly visible. The area of the step response is framed in black for illustration and can be seen again in high resolution in the right part of the figure.
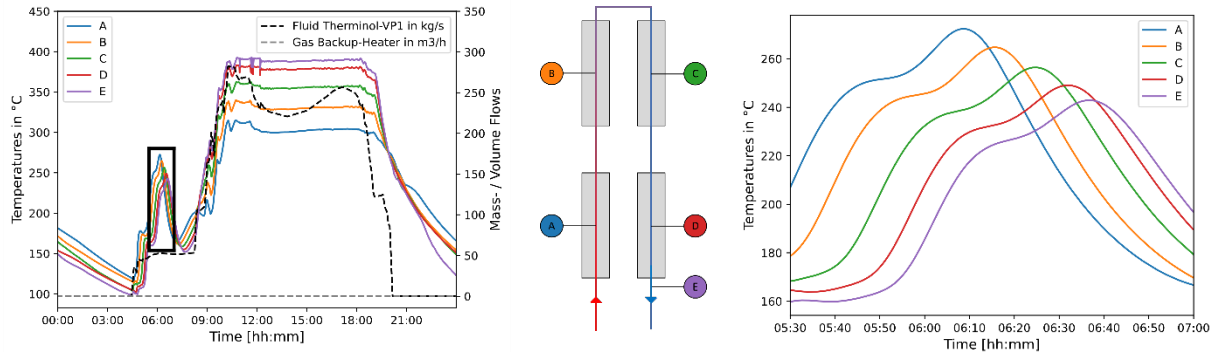
Figure 2. *Scheme of a PTC loop with four SCAs and five temperature sensors (center) as well as corresponding measured temperatures during one example day and one example loop of a commercial CSP plant (left) – framed thermal step response also shown in high resolution (right)*

For a temporally and spatially constant mass flow $\dot{m}$ and a qualitatively identical profile of temperatures measured at two temperature sensors with a temperature difference of ΔT, the heat loss $\dot{Q}_{\mathrm{L}}$ of the HTF between the respective sensors is calculated as follows:

$$\dot{Q}_{\mathrm{L}} = \dot{m} \cdot \overline{c_{\mathrm{p}}} \cdot \Delta T \tag{1}$$

Where $\overline{c_{\mathrm{p}}}$ corresponds to the average specific heat capacity of the HTF.

As can be seen in Figure 2 (right), the temporal temperature profiles at the different sensors are not identical but change with increasing flow direction and flow time. Due to heat conduction and turbulent mixing within the HTF, heat is also transferred within the HTF from the higher temperature section to the colder part of it in surrounding areas, as can be seen in a relatively narrow temperature profile at the loop inlet and a wider temperature profile at the loop outlet. As a result, not all the temperature reduction is caused by heat losses. In this work the simplified assumption is made, that the described internal heat transfer within the HTF and the resulting change in the temperature profile occurs in an identical way for all loops. As in the context of this work only relative heat losses of different loops to each other are considered, the influence of the internal heat transfer of the HTF on the vacuum loss determination can be neglected. The calculation of the heat losses in the context of this work is thus carried out using equation 1.

2.2 Calculation of temperature reduction and mass flow rate

Since the mass flow and the temperature reduction according to equation 1 are, in addition to material properties, the relevant factors for calculating the heat loss, these two quantities are determined. Figure 3 shows the measurement of temperature reduction and mass flow based on temperature profiles of a thermal step response. While the temperature reduction can be determined directly through the change in the respective temperature levels (black dashed lines), the underlying mass flow is determined by the ToF method (red dashed lines) [5].
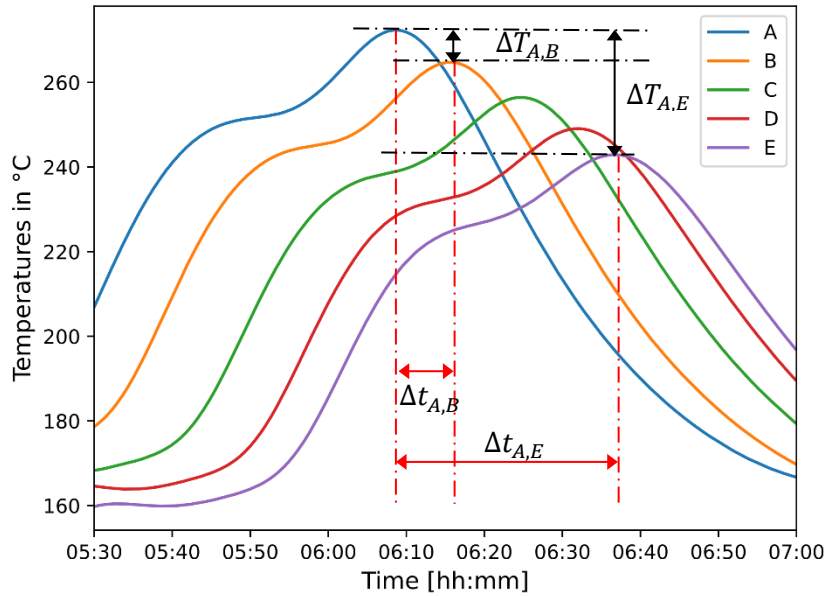
Figure 3. *Measurement of temperature reduction (quantitative shift, black dashed lines) and mass flow (temporal shift, red dashed lines) of a thermal step response during preheating of a commercial PTC plant*

In the ToF method, the time offset $\Delta t_{i,j}$ of the temperature profiles between sensors i and j is used to determine the velocity of the HTF. The corresponding mass flow rate is calculated with the inner tube diameter d of the tube and the integrated mean density $\overline{\rho(\vartheta_i, \vartheta_j)}$ as follows:

$$\dot{m}_{i,j} = \frac{\Delta l_{i,j}}{\Delta t_{i,j}} \cdot \frac{\pi}{4} d^2 \cdot \overline{\rho(\vartheta_i, \vartheta_j)} \tag{2}$$

The ToF method for the determination of mass flow distributions in CSP plants with PTC is described in detail by a separate work [5], measuring 94% of the data within an uncertainty of ± 5% of full scale. The general conditions for mass flow determination given in [5] are also assumed in this work and are as follows:

1. Uniform thermal step response through sensors
   - No additional external heat source or sink superimposing the thermal step response (e.g. electrical/thermal heater or fluctuant DNI on collectors)
   - Constant mass flow between first and last temperature measurement
2. The associated loop must be in operation and must not be hydraulically locked
3. Known or equal geometries and sensor positions of the corresponding loops

2.3 Vacuum loss determination

Based on the calculated temperature reduction and mass flow of all loops in the solar field, loops with an increased probability of vacuum loss are detected in two steps:

1. Comparison of the calculated heat loss in a single loop qualitatively to the average heat loss in the entire solar field
2. Comparison of the mass flow rate in a single loop with the mean mass flow rate in the entire solar field

Since convective heat loss increases with increasing flow velocity [6] (and thus with increasing mass flow rate), loops with increased heat loss at a reduced mass flow rate have an increased probability of vacuum loss. The recommended instructions for the operating personnel according to the results of the previous steps can be summarized as shown in Figure 4.
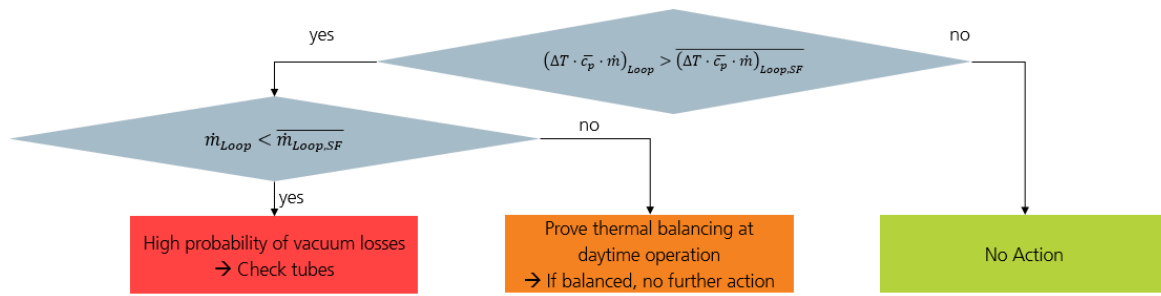
Figure 4. *Operational recommendations depending on determined heat loss and mass flow in a PTC loop of a commercial CSP plant.*

3. Operational Data Analysis

For this study, operational data was considered from the CSP plant Andasol III, located near Guadix, southern Spain. The power plant has a nominal turbine capacity of 50 MW and an estimated annual output of more than 165 GWh, generated by a generator coupled to the upstream steam turbine. Additionally, there is a two-tank thermal storage system with a capacity of approximately 30,000 tons of salt, which allows continuous power generation even during periods of fluctuating DNI or after sunset. The heat required for the power generation is supplied by a parabolic trough collector (PTC) solar field, divided into four subfields aligned with the cardinal directions: NW, NE, SE, and SW. Each subfield consists of 38 individual loops, totaling 152 loops for the entire solar field. As shown in Figure 2, each loop consists of four SCAs connected in series. Figure 5 provides an aerial view of Andasol III, illustrating the four subfields and their respective cold and warm header pipes. [7]

Figure 5. *Aerial view of Andasol III, including the four subfields and their respective cold and warm header pipes [8].*

The data on which this work is based on is identical to the analyzed data in [5], consisting of operational data from 15 consecutive days in September 2019 with a temporal resolution of less than 10 seconds. Eight of these 15 days meet the requirements specified in 2.3 and were thus used for the presented method. Figure 6 shows the temperature reduction and the mass flow for each loop as relative deviation from the mean of all loops over the considered 8 measurement days. It also shows analogously the heat loss (see. eq. 1), averaged over the 8 measurement days considered, for loops with both increased heat loss and reduced mass flow.

Loops with low mass flow rates often show a high temperature reduction. This is in line with expectations according to equation 1. The highest heat loss shown in Figure 6 – and thus the highest probability of vacuum losses according to the method presented – has Loop 34 (X-position = 9, Y-position =2, highlighted by a green frame), which has a high temperature reduction without having a strongly reduced mass flow.
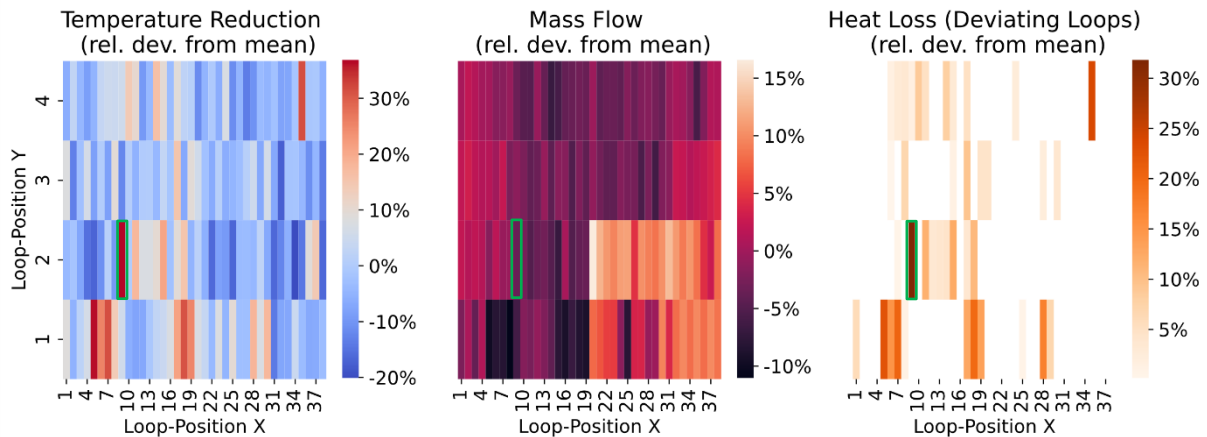

Figure 6. *Temperature reduction (left) and mass flow (center) for each loop as relative deviation from the mean of all loops, and heat losses (right) as relative deviation from the mean for loops with increased heat losses and decreased mass flow.*

As can be seen in Figure 6, loops with an increased probability of vacuum losses can be detected. To validate the results, the glass encasements of the corresponding loops (refer to Figure 1) can be subsequently checked for elevated temperatures and hence vacuum losses, either via infrared camera or direct temperature measurement using additional temperature sensors. By replacing affected collectors early on, there is potential to improve predictive maintenance and thus increase the efficiency of the entire CSP power plant.

4. Conclusion and Outlook

In this work it was shown, that by only analyzing the available operational data of the existing temperature sensors of a commercial CSP plant, it is possible to determine loops that have higher heat losses and thus a higher probability of vacuum losses. The determination of the heat losses is based on the measurement of temperature reduction and mass flow of a thermal step response between different temperature sensors during preheating of the solar field. The possible spatial resolution of the presented method is determined by the resolution of the existing temperature sensors in the solar field. In addition to the resolution shown at loop level, a resolution at SCA level is also possible.

In addition to consider only the maximum of the corresponding temperature profiles, a consideration of the integrated heat quantity of the thermal step response is also possible to further improve the accuracy of the described method. Since the results shown are based on the evaluation of real operating data at reduced mass flow during the night, an investigation at full, nominal mass flow is also considerable.

Mass flow determination via analysis of the thermal step responses with temperature sensors (ToF method) has already been validated in a previous work [5]. The validation of the presented results from combined measurement of mass flow and temperature reduction for vacuum loss detection is still pending. Possible approaches for a validation are either a direct

measurement of the glass surface temperature or the measurement of its resulting thermal radiation by means of infrared cameras for the corresponding collectors.

As the presented non-invasive method is simple, safe and cost effective, it has a high potential to increase the solar field efficiency due to early heat loss detection as a strong indication for vacuum losses and the resulting possibility for predictive maintenance of affected absorber tubes.

Data availability statement

The data used in this work comes from third parties. For reasons of confidentiality, they are not publicly accessible.

Author contributions

Thomas Kraft:	Conceptualization, Data curation, Formal analysis, Methodology, Validation, Visualization, Writing – original draft
Gregor Bern:	Funding acquisition, project administration, Supervision, Writing – review & editing
Shahab Rohani:	Writing – review & editing
Mark Schmitz:	Methodology, Writing – review & editing
Werner Platzer:	Supervision, Writing – review & editing

Competing interests

The authors declare that they have no competing interests.

Funding

Acknowledgement

References

[1] E. Setien, R. López-Martín, and L. Valenzuela, "Methodology for partial vacuum pres-sure and heat losses analysis of parabolic troughs receivers by infrared radiometry," In-frared Physics & Technology, vol. 98, pp. 341–353, 2019, doi: 10.1016/j.infrared.2019.02.011.

[2] T. Zoschke, S. Rohani, T. Fluri, Q. Hu, and Q. Fang, "Parabolic trough plant perfor-mance in China with focus on comparison of heat transfer fluids HELISOL®5A and Therminol® VP-1," in SOLARPACES 2017, Santiago, Chile, 2018, p. 130017.

[3] O. Arés-Muzio et al., "Characterization of thermal losses in an evacuated tubular solar collector prototype for medium temperature applications," Energy Procedia, vol. 2014, no. 57, 2121 - 2030.

[4] G. Espinosa-Rueda, J. L. Navarro Hermoso, N. Martínez-Sanz, and M. Gallas-Torreira, "Vacuum evaluation of parabolic trough receiver tubes in a 50 MW concentrated solar power plant," Solar Energy, vol. 139, pp. 36–46, 2016, doi: 10.1016/j.solener.2016.09.017.

[5] Kraft et al., "Mass Flow Distribution Measurement in Concentrated Solar Power Plants via Thermal Time-of-Flight Method," Solar Energy, vol. 273, p. 112486, 2024, doi: 10.1016/j.solener.2024.112486

[6] V. Gnielinski, VDI-Wärmeatlas: [Berechnungsunterlagen für Druckverlust, Wärme- und Stoffübertragung], 10th ed. Berlin, Heidelberg [u.a.]: Springer, 2006.

[7] Marquesado Solar, Andasol 3 Power Plant. [Online]. Available: https://marquesadosolar.com/plant-andasol-3/ (accessed: Aug. 22 2023).

[8] S. Rohani, "Modelling, Simulation and Data Validation of a Solar Thermal Parabolic Trough Plant with Storage," Master Thesis, Fraunhofer Institute for Solar Energy Sys-tems (ISE), Faculty of Mechanical, Electrical and Industrial Engineering, Brandenburg University of Technology Cottbus-Senftenberg, 2015.